



Geochemical and mineralogical evaluations of coal, shale, and mine waste overburden from Makum coalfield of the Northeast India

Nilotpol Bhuyan¹ · Nazrul Islam^{1,2} · Monikankana Saikia^{1,2} · James C. Hower³ · Binoy K. Saikia^{1,2}

Received: 13 February 2023 / Revised: 5 April 2023 / Accepted: 26 June 2023
© The Author(s) 2023

Abstract

The Cenozoic-age Makum coal from northeastern India offers numerous research opportunities because of its diverse geochemical and geological characteristics. Due to its high sulfur content, the coal has been found to be less useful for industrial purposes. It can, however, serve as a hub for ongoing research on coal-based derivative products. The aim of this research work is to investigate the mineralogical and geochemical compositions of the coal, mine overburden (MOB) and shale samples taken from the Makum coal field and also on establishing a mutual relationship between them. To characterize the geochemical controlling factors of the Makum coal field, the study employs coal petrography, FTIR, mineralogical, and geochemical analysis. According to X-ray diffraction analysis, the major minerals like quartz, kaolinite, haematite, illite, pyrite, and calcite are present in coal and MOB. Pyrite is observed by SEM–EDS analysis as cubic-shaped particles that are smaller than a few μm in size. The presence of sulfide minerals represents a phase of pyrite mineralization. The petrography study was used to better understand the environment that existed during the formation of the plant material, which aids us in determining the quantity of detrital mineral sediment contained in the coal. According to the ICP-MS analysis, the samples indicate significant levels of rare earth elements including yttrium. The present study reveals higher concentrations of potential hazardous elements in the coal samples, with V, Cr, Ni, Cu, and Zn content in coal being considerably enriched compared to world-average concentrations. The correlation analysis reveals that the potential hazardous elements like Co, Ni, As, and Cu are associated with pyrite as they have strong affinity towards pyrite. Thus, numerous minerals and rare earth elements (REEs) exist, opening up a fresh avenue for more research in the area. This study also assists researchers in understanding the significance of Makum coal and provides numerous ideas for coal characterization.

Keywords Coal geology · Mine waste overburden (MOB) · Petrology · Rare earth elements (REEs) · Potentially hazardous elements (PHEs)

1 Introduction

Coal, a combustible sedimentary rock originating from ancient vegetative matter, has a diverse range of organic and inorganic components that contributed to its creation and post-depositional actions that account for its structure and metamorphism (Dai et al. 2020). Australia, Russia, China,

India, and the United States have the largest coal deposits. Coal is utilised in the production of energy as well as in industrial applications such as cement, iron, steel, chemicals, and fuels (Oxford Analytica 2017). The bulk of coal is used to create electricity, which today accounts for 40% of worldwide energy consumption (IEA 2020, 2022).

The discovery of large coal deposits in the northeastern region (NER) of India over the years has sparked interest in its potential for several sectors. Because of the significant quantity of sulfur present in these NER coals, in the power and industrial sectors, they are less prevalent. Sulfur compositional differences in coal are mostly influenced by sedimentary settings during peat deposition and post-depositional modifications (Chou 2012), particularly the sulfate in the saltwater that inundated the peat swamps. Sulfur and several trace elements in coal undergo major changes during

✉ Binoy K. Saikia
bksaikia@neist.res.in; bksaikia@gmail.com

¹ Coal and Energy Division, CSIR-North East Institute of Science and Technology, Jorhat, Assam 785006, India

² Academy of Scientific and Innovative Research (AcSIR), Ghaziabad 201002, India

³ Center for Applied Energy Research, University of Kentucky, 2540 Research Park Drive, Lexington, KY 40511, USA

coal combustion and lead to atmospheric pollution (Mukherjee and Srivastava 2005; Rabha et al. 2018; Islam et al. 2020). Northeastern India coals have a high yield of vitrinite and volatile matter, yielding double the amount of tar in comparison to other Indian coals (Baruah and Khare 2010). With the world becoming more environmentally conscious, coal-based industries are in jeopardy due to the harm that coal ash and acid mine drainage inflict in rivers and streams. In India, according to the Indian Bureau of Mines, 755,440 hectare (ha) (7554.4 km²) of land is under mining lease with 5% [approximately 37,772 ha (377.7 km²)] actively mined (Juwarkar and Jambhulkar 2008; Indian Bureau of Mines (IBM) 2001). The coal mining activity also generates a large volume of mine waste containing rock, shale, and different types of soil along with minerals and potentially hazardous elements. These coal and mine wastes, termed as mine overburden (MOB), mainly have high sulphur content (2%–12%, as received basis) in the Makum coal fields of northeast India. The coal mining activity leads to major changes in water bodies through generation of acid mine water, soil topography, soil erosion, retardation of plant growth, and environmental pollution (Islam et al. 2021; Dutta et al. 2017). Coal associated with some higher concentrations of potentially hazardous elements such as lead (Pb), zinc (Zn), cadmium (Cd), mercury (Hg), chromium (Cr), arsenic (As), Nickel (Ni), etc. and the mining activity or improper utilization of coal may cause severe health problems (Dutta et al. 2020). Dutta et al. (2020) reported that the presence of potentially hazardous elements in coal can cause cytotoxic to both human and animal during the exposure of higher concentration (300 µg/ml). The elemental and mineralogical studies in coal samples provide information about the paleoenvironment of coal formation, along with formational and regional history, mode of occurrence and their identification with potential mobility of particular trace elements. The mineralogical study also helps in evaluation of the behavior of different coals in the preparation and utilization processes (Saikia et al. 2015b). Therefore, the investigation of the distribution of elements and mineral matter present in any coals are of prime importance not only for its geochemical study but also for clean coal initiatives. In earlier studies, some of the physico-chemical characteristics of coal and mine waste over burden from Ledo and Tirap colliery of Makum coalfield were established (Islam et al. 2021; Dutta et al. 2017), however, comprehensive geochemical and mineralogical investigations have not been performed by using advanced analytical techniques.

The main objective of the present research work is to evaluate the mineralogy and geochemistry of coal, shale, and MOB collected from the Tirap, Tikak, and Tipong collieries of the Makum coalfield. This study evaluates the petrological analysis of coal samples that may lead us to

the identification of coal depositional environment and their nexus among India's major coalfields. Due to the growing application of rare earth elements (REEs) in modern civilization, finding alternate sources of the REEs recovery is a topic of high interest. The major novelty of the present study is to determine the distribution of REEs and potentially hazardous elements (PHEs) in coal, MOB, and shale samples of Makum coalfield. This study also focuses on the relationship among the major trace and rare earth elements that may offer additional insight into the origin of these elements.

2 Material and methods

2.1 Geological characteristics of the study site

The Makum coalfield, which stretches from 27°15' to 27°25'N latitude and 95°40' to 95°50'E longitude along the western most side of the Patkai range, is one of the most important coalfields in NE India. Out of the five mining sites of the coal field, Tikak and Tirap have open-cast mines, whereas Baragolai, Ledo, and Tipong have underground mines. The Oligocene Tikak Parbat Formation, which consists of alternating sandstone, siltstone, mudstone, carbonaceous shales, and coal seams, is where all of the coal beds are found. A linear "Belt of Schuppen" overthrusts run through the whole region. The lithological composition of the Tikak Parbat formation (Stratigraphic succession is presented in Table 1) is characterized by the massive to well-bedded, fine to medium grained, yellowish to light grey, and greyish white sandstones which are entrapped with shale and coal seams. Two thick, commercially viable coal seams occur in the lower part of the segment. The base of the lowest seam, which goes by the name of the "18 m" seam, delineates the conformable boundary between the Baragolai and Tikak Parbat Formations (Evans 1932) The "6 m" seam is located at a higher elevation in the section. These seams are coal-rich units with occasional siliciclastic partings rather than continuous deposition of pure coal. According to Ahmed (1996), the coals are categorised as high volatile B bituminous, which denotes a level of maturation connected to the local tectonics.

2.2 Analytical characterization

2.2.1 Sampling program

Using Standard method (ASTM 2010), coal samples were collected from one of the largest coal mines in the Makum coalfield. The rock types were mainly sandstone, shale, and carbonaceous clay. Several coal, MOB, and shale samples were gathered from three distinct sites (shown

Table 1 Geological succession of the coalfields of the foreland basin (modified after Raja Rao 1981)

Age	Group and formation	Thickness (m)	Rock types
Pliocene	Dihing Group	1800	Mostly pebbly sandstone with thin greyish clay beds
<i>Unconformity</i>			
Mio-Pliocene	Namsang Formation	800	Fine to coarse grained sandstone with bands of clay
<i>Unconformity</i>			
Miocene	Tipam Group	1800	Mottled clay with greyish soft sandstone Ferruginous, fine to coarse grained micaceous to felspathic sandstone
	(1) Girujan Clay (2) Tipam Sandstone	2300	
<i>Unconformity</i>			
Oligocene	Barail Group	600	Greyish to yellowish white sandstone, sandys shale, coal seams Greyish to bluish grey or yellowish red mudstone, shale, sandstone, carbonaceous shale and thin coal seam Compact, fine grained, dark grey sandstone with bands of splintery shale
	(1) Tikak Parbat Formation	3500	
	(2) Baragolai Formation (3) Naogaon Formation	2200	
Eocene	Disang Group	3000	Splintery dark grey shales and thin sandstone interbands

in Fig. 1) of the area. Three main locations were used to gather the samples are Tirap, Tipong, and Tikak colliery. All of the coal samples from the Tirap colliery were labelled as NBTP-1, NBTP-2, NBTP-3, NBTP-4, and NBTP-5. Similarly, one coal sample named TPM (1) and one shale sample named TPCS from the Tipong colliery. From Tikak area TPC 20 was labelled as a coal sample, while TPOB20 and TPOB60 were designated as MOB.

2.2.2 Proximate and ultimate analysis

The proximate analysis and the forms of sulfur analysis were carried out using the appropriate ASTM standard procedures (ASTM 2011a, b, c). The proximate analysis of the coal sample was done in the ‘Proximate Analyzer’ (Model: TGA 701; Leco Corporation, USA) by following the ASTM method. The carbon and hydrogen were estimated by using ‘Elemental Analyzer’ (Model: Perkin–Elmer 2400).

2.2.3 SEM analysis

Scanning electron microscopic analyses were also performed on the raw coal and MOB samples. The samples were coated with platinum by Auto Fine Coater and examined in a scanning electron microscope of model No. ZEISS, SIGMA, Make: Carl ZEISS Microscopy, Germany. Observations and photographs with the SEM were made at

20 kV with a working distance of 11 mm and spot size 36. The SEM images were further developed by using ‘Image J’ program (software version 1.47).

2.2.4 Determination of forms of sulfur

ASTM 2002 technique was used in the current study to determine the different forms of sulfur. Only two of sulfur's three forms, sulfate and pyritic, are directly measured in this process. Organic sulfur, calculated by difference, is the third form:

$$\text{Organic sulfur} = \text{Total sulfur} - (\text{Sulfate sulfur} + \text{Pyritic sulfur}) \quad (1)$$

The total sulfur content of the coal sample was measured using a Leco S-144 DR dual range sulfur analyzer.

2.2.5 Petrographic characterisation

For petrology, the coal was crushed to a top size of 20 mesh (840 µm); encased as epoxy-bound particulate pellets; prepared to a final 0.05-µm alumina polish; and examined with a 50×, oil-immersion, reflected-light objective. Description of the coal samples with nomenclature following the terminology recommended by the International Committee for Coal and Organic Petrology (ICCP) for vitrinite (ICCP 1998), inertinite (ICCP 2001), and liptinite (Pickel et al. 1994). The measurement of vitrinite reflectance was carried out using the appropriate ASTM standard.

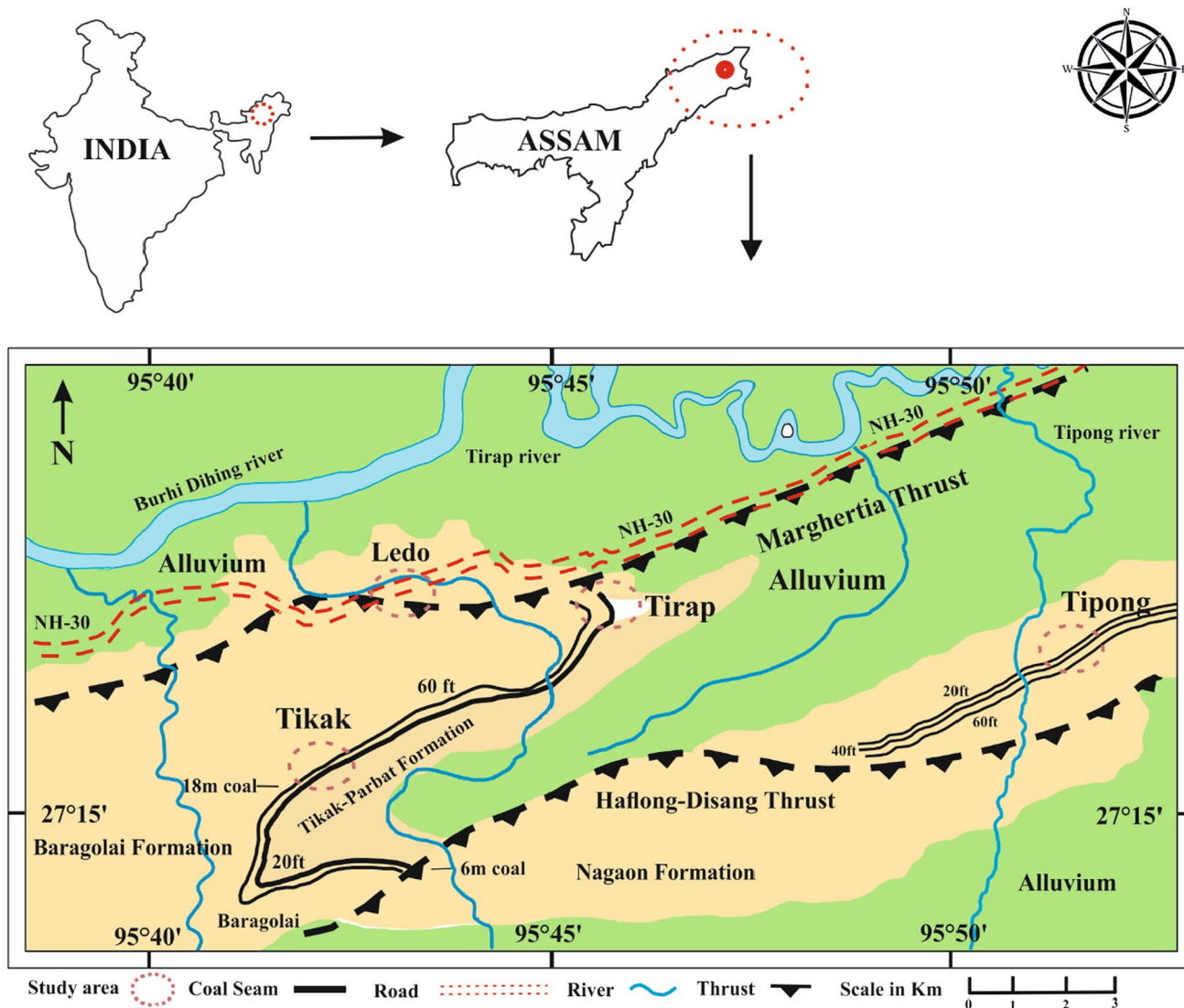


Fig. 1 Makum Coal Basin regional geological map, Assam, India, modified after Ahmed (1996)

2.2.6 Elemental analysis (ICP-MS) of coal

The trace and REEs concentrations in coal and MOB samples were quantified by using the High Resolution Inductively Coupled Plasma Mass Spectrometer (Element XR; Model: ThermoFisher Scientific). Collision/reaction cells (Q Cell technology) of ICP MS was also used to determine some selected ions present in coal and MOB samples. The recommended ASTM procedure was applied for sample digestion and further analytes determination (ASTM 2021). A microwave-induced combustion (MIC) procedure was applied for coal digestion for subsequent

determination of As, Cd, and Pb by inductively coupled plasma mass spectrometry (ICP-MS) and Hg using cold vapor (CV) generation coupled to ICP-MS. Pellets of coal (500 mg) weighed and transferred together the filter paper to the quartz holder of MIC system.

2.2.7 FTIR analysis

The presence of functional groups in each coal and shale sample was detected by the Fourier transform infrared (FT-IR) spectroscopy using the potassium bromide (KBr) powder method. The coal samples were mixed with KBr in

the ratio 1:100 and then converted them into pellets using a hydraulic press. The FTIR spectrum thus generated was then recorded from wavenumber; 4000–400 cm⁻¹ in transmittance mode (*T*, %). The scanning was done using the FTIR spectrophotometer (Model: Spectrum Two, Make: Perkin Elmer). Attenuated Total Reflection Fourier Transform Infrared spectroscopic (ATR-FTIR) analysis of MOB was carried out in an FTIR spectrometer (Spectrum-Two; Perkin Elmer) in the range of 400–4000 cm⁻¹ to determine the functional group present.

2.2.8 X-ray diffraction (XRD) analysis

The raw samples were analyzed using an X-ray diffractometer (Rigaku, Ultima IV) in accordance with the technique described elsewhere (Islam et al. 2019). The materials' X-ray diffraction data were collected using a starting angle of 2.00° and a stopping angle of 90.00°, as well as a step angle of 0.02° and a scanning rate of 1° C/min, with a target Cu Kα (1.54056Å). Mineral peaks were identified using the library database 'Rigaku PDXL 1.2.0.1' application.

2.2.9 X-ray photoelectron spectrometer (XPS) analysis

The X-ray photoelectron spectrometer (XPS) analysis was carried out to determine the surface structure and composition of coal, mine overburden and shale samples.

The analysis was performed with a Thermo-Scientific ESCALAB Xi⁺ spectrometer using a monochromatic Al Kα X-ray source (1486.6 eV) and a spherical energy analyzer that operates in the constant analyser energy (CAE) mode using the mode of the electromagnetic lens. The CAE for high-resolution spectra is 50 eV and that for survey spectra is 100 eV.

3 Results and discussion

3.1 Physico-chemical analysis

Table 2 shows the physico-chemical properties of the coal and the two mine overburden samples (TPOB 20, TPOB 60). Low amounts of moisture content are present in the coal samples, with the MOB sample having the greatest level (3.38%, as received basis) and the coal sample having the lowest level (0.97%) (NBTP-3). The fixed carbon analysis shows 60.03% and 15.53% as highest and lowest values and the volatile matter (VM) varies from 46.22% to 13.22% for the samples. The MOB shows only 9.52% carbon content, but the coal samples show medium to moderate carbon level (as received, 66.3%–81.1%). Furthermore, they exhibit a very low hydrogen content (ranging from 1.77% to 5.12%).

The five samples (TPC 20, TPM 1, TPOB 20, TPOB 60, and TPCS) were also examined for the distribution

Table 2 Physico-chemical properties of the coal MOB, and shale samples (as received wt%)

Sample	Proximate analysis				Ultimate analysis	
	M	VM	Ash	FC	C	H
NBTP-1	1.02	40.61	9.02	49.35	66.4	3.99
NBTP-2	1.26	37.33	9.77	51.64	71.4	4.98
NBTP-3	0.97	34.27	8.65	54.27	67.3	4.85
NBTP-4	1.37	33.34	11.02	54.27	68.3	4.97
NBTP-5	1.47	30.74	7.76	60.03	69.4	5.12
TPM-1	1.84	46.22	3.02	48.91	72.3	3.89
TPC 20	3.18	42.38	2.92	51.52	81.1	5.69
TPOB 20	3.35	13.22	67.90	15.53	9.52	1.77
TPOB 60	2.73	12.78	71.22	13.26	7.32	1.54

Note: *M* moisture, *VM* volatile matter, *FC* fixed carbon, *C* carbon, *H* hydrogen

Table 3 Forms of sulfur analysis of coal, MOB, and shale samples (as received wt%)

Samples	Total sulfur (S) (wt%)	Pyritic sulfur (wt%)	Sulfate sulfur (wt%)	Organic sulfur (wt%)
TPC-20	2.30	0.52	0.10	1.68
TPM-1	2.84	0.72	0.21	1.91
TPOB-20	2.63	0.86	1.07	0.70
TPOB-60	2.47	0.55	0.81	1.11
TPCS	0.40	0.17	0.21	0.02

of various forms of sulfur. The coal samples exhibit relatively high volatile matter and moderate content characteristics. The forms of sulfur obtained are shown in the Table 3. The current samples have a total sulfur content ranging from 0.40% to 2.84% (wt%), of which 27%–73% is organic. There is pyritic sulfur present, ranging from 25% to 42.5% of the total sulfur. The distribution of pyritic sulfur does not follow any regular pattern in these coals. Sulfur distribution studies aid in the exploration and selective mining of coals, as well as providing information on deposition conditions. However, detailed basin analysis including paleoclimate, surface and ground water, and tectonic accommodation, in some cases indicate that high sulfur content in coal may not be solely a function of marine

influence (Greb et al. 2002; Turner and Richardson 2004). In the absence of detail basin analysis and temporal factors, the influx of sulfur from other sources cannot be commented upon at present.

3.2 Petrology of the coal samples

Table 4 shows the maceral compositions of the seven coals. We collected coal samples from all three study sites, and the maceral makeup of the analyzed samples is essentially the same. On a mineral-free basis, all of the current coals contain more than 92% vitrinite. The vitrinite is dominated by the telovitrinite which, in turn, has abundant collotelinite. The inertinite groups consists

Table 4 Macerals and minerals in coal (vol%), plus maximum and random vitrinite reflectances (R_{\max} and R_{random} , %)

Maceral	NBTP 01	NBTP 02	NBTP 03	NBTP 04	NBTP 05	TPM-1	TPC 20
Telinite	9.1	10.1	5.1	8.9	10.6	13.9	3.9
Collotelinite	63.0	65.2	68.6	60.5	68.8	57.1	72.7
Total telovitrinite	72.1	75.3	73.7	69.3	79.4	71.0	76.5
Vitrodetrinite	14.3	11.3	14.9	22.6	12.6	14.5	17.0
Collodetrinite	0.0	0.0	0.0	0.0	0.0	0.0	0.0
Total detrovitrinite	14.3	11.3	14.9	22.6	12.6	14.5	17.0
Corpogelinite	1.4	1.2	0.9	0.3	1.1	0.3	0.6
Gelinite	0.0	0.3	0.0	0.0	0.0	0.8	0.6
Total gelovitrinite	1.4	1.5	0.9	0.3	1.1	1.1	
Total vitrinite	87.7	88.1	89.4	92.3	93.1	86.6	94.2
Fusinite	1.0	0.3	0.3	0.6	0.0	0.5	0.3
Semifusinite	3.0	1.2	1.1	0.3	0.3	0.0	0.3
Micrinite	0.0	0.3	0.0	0.0	0.0	0.0	
Macrinite	0.4	0.0	0.3	0.0	0.0	0.5	
Secretinite	0.0	0.0	0.0	0.0	0.0	0.0	
Funginite	0.0	0.9	1.7	4.6	1.7	1.4	
Inertodetrinite	0.0	0.0	0.0	0.0	0.0	0.0	
Total inertinite	4.4	2.7	3.4	5.4	2.0	2.5	1.0
Sporinite	1.4	0.6	0.6	0.9	1.4	0.0	1.6
Cutinite	0.6	0.0	0.0	0.0	0.9	0.8	
Resinite	1.0	1.2	0.9	0.9	0.9	1.6	
Alginite	0.0	0.0	0.0	0.0	0.0	0.0	
Liptodetrinite	0.2	0.0	0.0	0.0	0.0	0.0	
Suberinite	0.0	0.0	0.0	0.0	0.3	0.3	
Exsudatinite	0.0	0.0	0.0	0.0	0.0	0.0	0.3
Total liptinite	3.2	1.8	1.4	1.7	3.4	2.7	0.6
Silicate	4.0	5.4	4.9	0.0	1.1	5.5	3.9
Sulfide	0.4	1.5	0.9	0.3	0.3	1.6	0.3
Carbonate	0.0	0.0	0.0	0.0	0.0	0.0	0.0
Other	0.4	0.6	0.0	0.3	0.0	1.1	0.0
Total mineral	4.8	7.4	5.7	0.6	1.4	8.2	0.3
Rmax	0.66	0.71	0.69	0.67	0.66	0.65	0.68
SD	0.04	0.05	0.06	0.03	0.03	0.05	0.04
Rrandom	0.64	0.67	0.65	0.63	0.61	0.63	0.64
SD	0.04	0.06	0.06	0.03	0.03	0.05	0.03

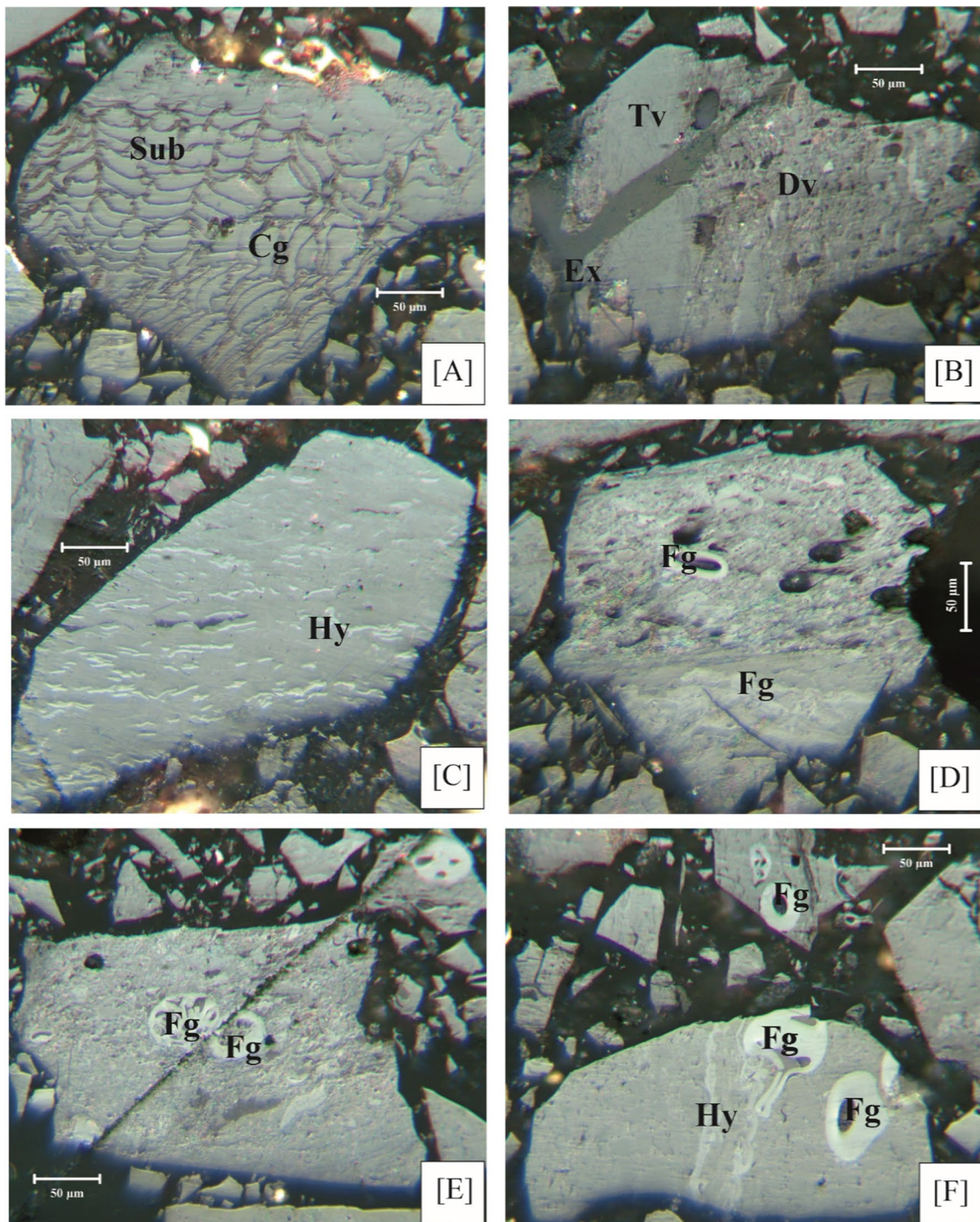


Fig. 2 Representative photomicrographs of macerals of Tirap colliery coals. Scale = 50 µm for all images. **a** Exsudatinite (ex) in telovitrinite (tv) and detrovitrinite (dv). **b** Suberinite (sub) and corpogelinite (cg).

c Fungal hyphae (hy) in vitrinite. **d** Funginite (fg) in macrinite/detrital-inertinite matrix. **e** Funginite (fg) in detrital vitrinite/inertinite/lip-tinite matrix. **f** Funginite as sclerotia (fg) and hyphae (hy)

of varying concentrations of fusinite, semifusinite, and funginite. Funginite occurs as sclerotia (Fig. 2d–f) and hyphae (Fig. 2c, f). Some sense of the complexity of the

maceral assemblages can be seen in (Fig. 2a, d) where the funginite occurs in detrital matrices. Liptinite occurs as sporinite, cutinite (Fig. 3a, b), suberinite (Fig. 3c, d),

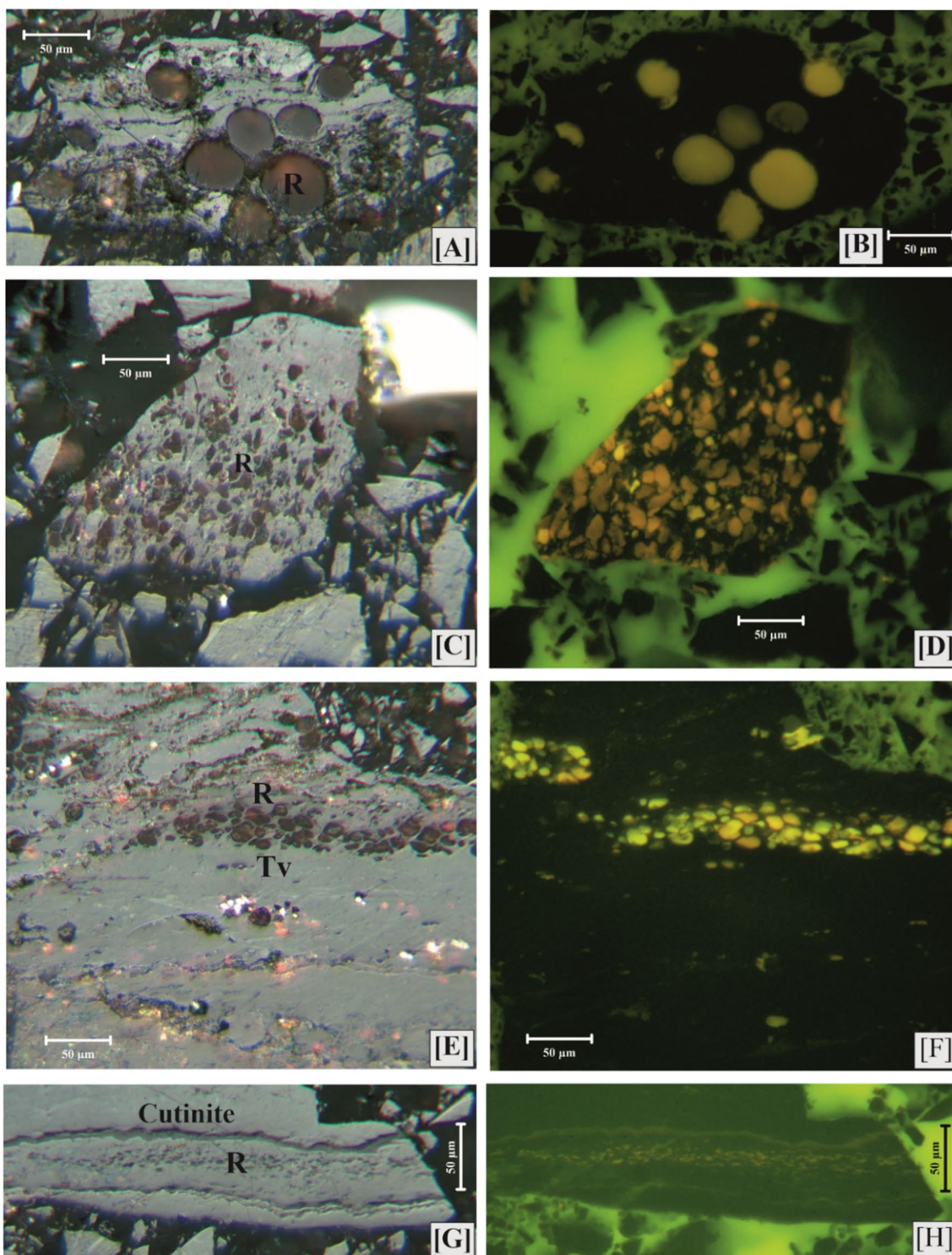


Fig. 3 **a** and **b** White-light and blue-light images of resinite (r). **c** and **d** White-light and blue-light images of resinite (r). **e** and **f** White-light and blue-light images of resinite (R) with telovitrinite (tv). **g** and **h** White-light and blue-light images of cutinite and resinite (R)

exsudatinites (Fig. 3e), and resinite (Fig. 3a). Resinite occurs within cutinite (Fig. 2a, b) and as clusters or layers in association with vitrinite (Fig. 3).

Samples with an R_{\max} of 0.65–0.71 percent are dominated by vitrinite (86.6%–95.2%), with collotelinites (69.3%–81.5%) being the most prevalent maceral

subgroup within the vitrinite group, followed by vitrodetrinite (11.3%–22.6%) and telinite (5.1%–13.9%) (Table 4). The mean random reflectance of the coal samples falls within the range for high volatile B bituminous coal, according to the International Standard for Coal Classification (Saikia et al. 2016). Comparing the vitrinite and R_{\max} values found in the Cenozoic age Makum coalfield to those found in other prominent coalfields in India of the Permian age shows that the Jharia coalfield in Jharkhand has 32.04%–74.90% vitrinite with $R_{\max} = 1.23\%$ – 2.03% (Saikia et al. 2016), and the Ib valley coalfield in Orissa has 4.5%–80.2% vitrinite (Senapaty and Behera 2015). The R_{\max} is an important coal rank measure that facilitates correctly evaluating changes in coal used for coke production. The presence of vitrinite in the coal samples tested suggests that the coal formed in a wet forest swamp, primarily from arborescent flora (Suwarna 2006; Suárez-Ruiz and Ward 2008; Solaymani and Taghipour 2012) Funginite and liptinite macerals were observed in the samples (Table 4; Fig. 2). Lesser amounts of inertinite (2.5%–5.4%) and liptinite (1.4%–3.4%) are also found in the coal samples in comparison to the Indian Permian Gondwana coals such as Jharia (inertinite 15.02%–51.40%, liptinite 0.02%–10.40%) and Ibvalley coalfield, Orissa (inertinite 12.5%–92.2%, liptinite 3.30%–22.2%) (Fig. 3a, c, f). Coals of Makum coalfield show varying proportions of vitrinite (92.7%–65.5%), liptinite (22.0%–0.6%), and inertinite along with mineral matter and shale or clayand were deposited under the influence of marine environment (Barooah and Baruah 1996).

Silicate, sulfide, carbonate, and other mineral phases are prevalent in the samples, with silicate having a maximum concentration of 5.5% in TPM (1) and a minimum concentration is observed in below detection limit for NBTP 04. Sulfides have been observed in lower concentrations, with a highest value of 1.6% in TPM 1 and lowest in NBTP04 with 0.4%. Because of their tiny size and close connection in most coals, determining sulfur in individual macerals is challenging. The total sulfur concentration of individual macerals isolated from two coals was determined to be the lowest in fusinite. The liptinite (mostly sporinite) has the most organic sulfur while inertinite contains the least, sulfur level in vitrinite macerals is moderate (Ward and Gurba 1998).

3.3 XRD mineralogy

XRD analysis was used to identify the principal minerals contained in coal samples (Fig. 4). The qualitative identification of minerals using XRD spectra in the coal

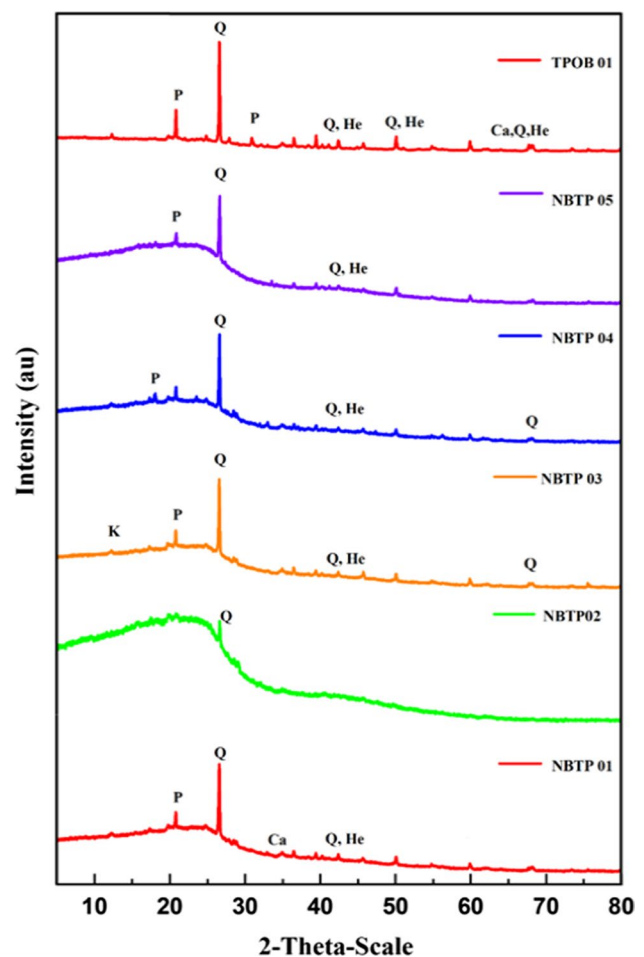


Fig. 4 Qualitative XRD-analysis of coal and MOB samples showing the presence of mineral phases (Q: Quartz; He: Haematite; P: Pyrite; Ca: Calcite; K: Kaolinite)

samples mostly comprises quartz (SiO_2), kaolinite ($\text{Al}_2\text{O}_3 \cdot 2\text{SiO}_2 \cdot 2\text{H}_2\text{O}$), hematite (Fe_2O_3), calcite (CaCO_3), and illite ($(\text{K}, \text{H}_3\text{O})(\text{Al}, \text{Mg}, \text{Fe})_2(\text{Si}, \text{Al})_4\text{O}_{10}[(\text{OH})_2 \cdot (\text{H}_2\text{O})]$), with quartz and hematite dominating the assemblages. Non-siliceous minerals, for instance pyrite (FeS_2), was observed. Additionally, the existence of mineral phases of detrital clay minerals, such as kaolinite, and silicate minerals can be deduced. The determined detrital clay minerals and silicate minerals are also supported by earlier studies (Saikia et al. 2015a, 2018; Rabha et al. 2018).

3.4 FTIR analysis of functional groups

The surface functional groups of raw coal, two MOBs, and one carbonaceous shale samples were examined using FTIR spectroscopy. Figure 5 depicts the FTIR analysis of the samples. The stretching vibration bands of S–S and

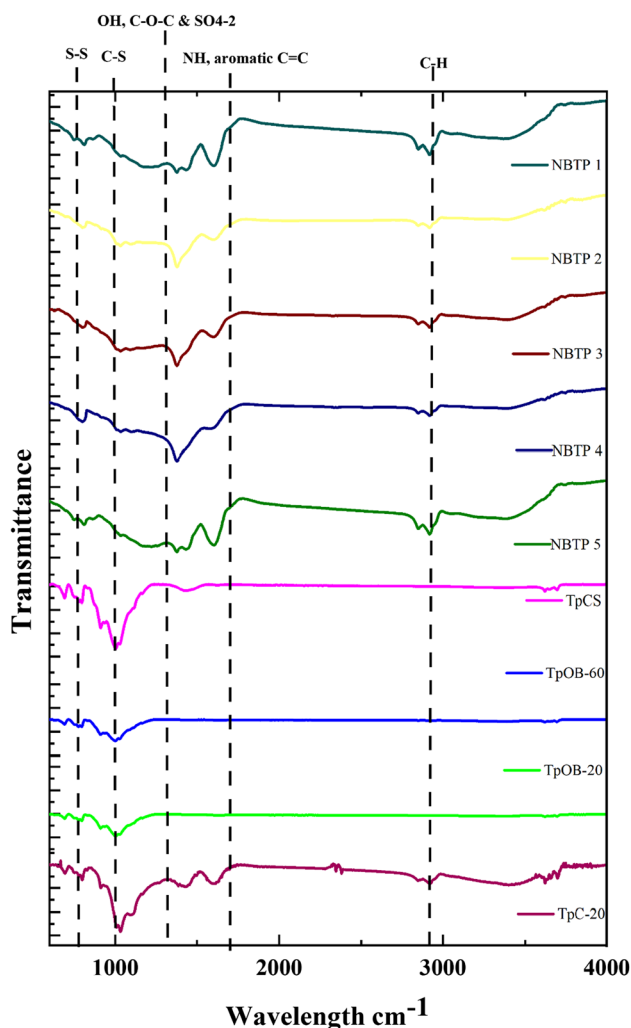


Fig. 5 FTIR analyses of raw coal, MOB, and shale samples showing the presence of functional groups

C–S bonds in primary and secondary thiols were determined to be 530 and 670 cm^{-1} , respectively. The absorption bands due to aliphatic alcohols, ether groups (O–H, C–O–C), and the SO_4^{2-} group occurs at the region of $1100\text{--}1005\text{ cm}^{-1}$. The aliphatic amino (NH), aromatic C=C, and aliphatic alkyl groups showed the absorption bands within the range of $1410\text{--}1615\text{ cm}^{-1}$ in TPM (1) and TPCS samples. In TPM (1), the aromatic C=C stretching vibrations ($1635\text{--}1600\text{ cm}^{-1}$) caused strong absorptions which indicate the presence of carbon content. The S–S and C–S, C–O–C, and SO_4^{2-} bonds are more prominent in the Tirap coal (TPM (1)). The peak at 2850 cm^{-1} , which appears as sharp peaks of medium intensity, may be assigned to aliphatic and alicyclic CH_3 , CH_2 , and CH

groups. However, major contributions are anticipated to be due to CH groups (Fig. 5).

3.5 Observations from SEM–EDS analysis

Figures 6 and 7 show SEM pictures of the minerals and carbonaceous structure in samples of coal, MOB, and carbonaceous shale. The particle size and shape distributions are erratic according to the SEM micrographs of the samples. The surface morphology revealed a non-uniform topography with minerals embedded in a carbon matrix. According to the elemental analysis, there are significant amounts of silicon, iron, aluminium, carbon, oxygen, and traces of sulfur. Pyrite was detected by SEM–EDS analysis in the form of particles with cubic shapes less than a few μm . EDS reveals the presence of the Si–Al clay mineral kaolinite. Gypsum was also confirmed by the SEM images. Its origin can be regarded as the weathering product of calcite with SO_4^{2-} derived from pyrite oxidation (Saikia et al. 2015a).

3.6 Abundance of elements in coal, MOB and shale samples

The result of the major and trace element data from representative samples of the study area are listed in Table 5. From the previous study (Saikia et al. 2015a), it has been reported that the major minerals associated with coals in the Northeast India include kaolinite, zircon, pyrite, goyazite, chlorite, xenotime, siderite, titanium oxide (anatase or rutile), iron-bearing gahnite, rhabdophane, carbonate, jarosite, illite, and mixed-layer illite/smectite. However, the coals are also found to be rich in F, Pb, Sr, Zr, and Ba. Earlier work confirmed the presence of element Cr, which is regarded as a marker or index element for the Oligocene coals of the Makum coalfield of Northeastern India (Mukherjee et al 1992). In our study, we have also observed a significant Cr concentration in the samples. Additionally, the coals have low concentrations of most other elements of environmental concern, such as Co, Mo, Mn, etc. Further it was also established that the Eocene and the Oligocene coals of Northeastern India originated under marine conditions. Sulfides, such as pyrite, in coal can be easily weathered; once the crystal lattice of pyrite is destroyed, trace elements with a sulfur affinity may be released into the environment. The origin of pyrite in coal has been attributed to the marine-influenced depositional environment with its the influx of SO_4^{2-} ions (Spears 2000).

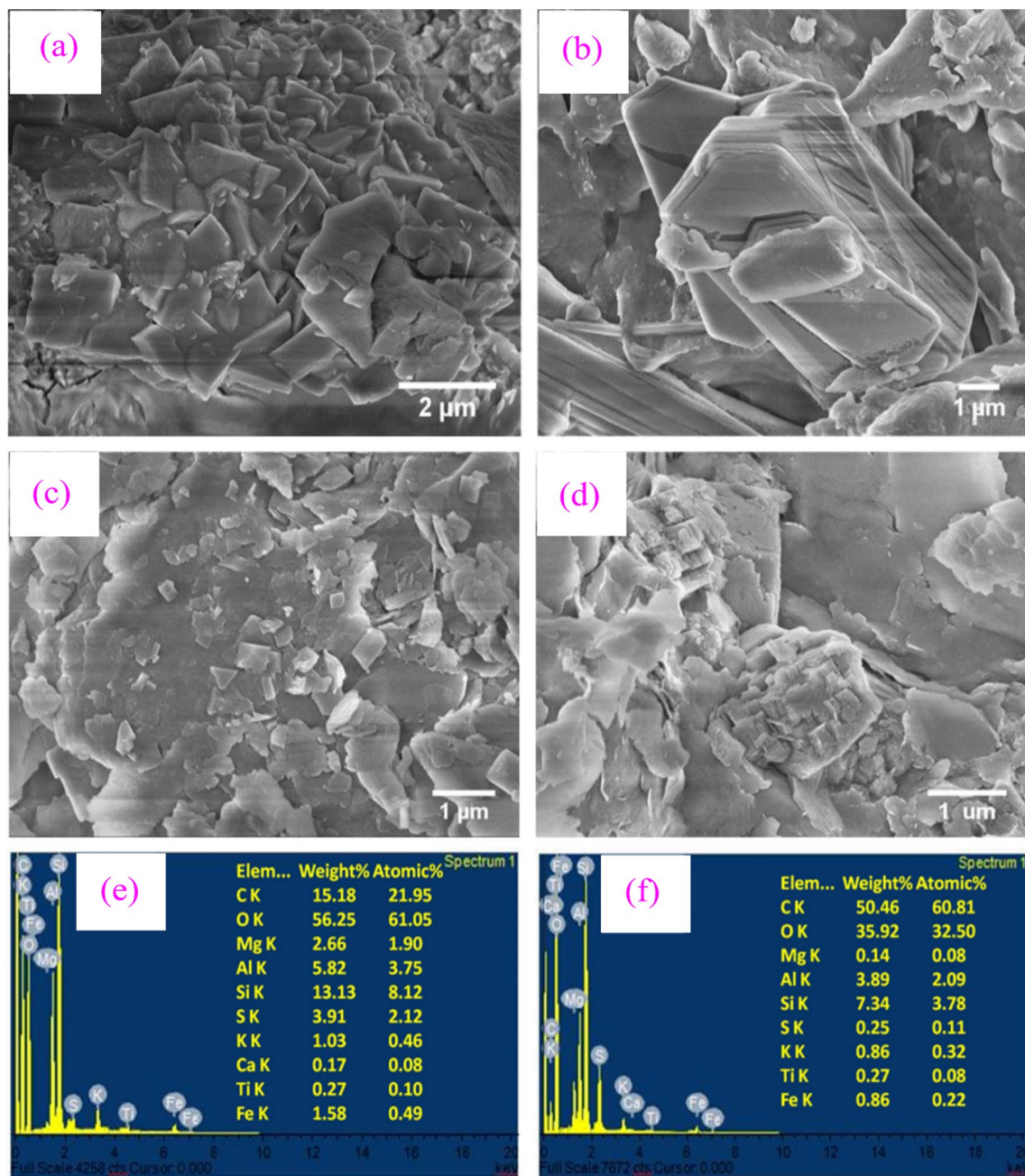


Fig. 6 SEM micrographs of **a** TPOB-20, **b** TPOB-60 samples, **c** TPM(1), and **d** TPC samples; **e** and **f** shows EDS analysis of TPOB-20 and TPOB-60, respectively. Presence of Fe-sulfide are seen in the morphology of the micrographs (see EDS analysis)

3.7 XPS analysis of Fe-bonding

XPS characterizations of the coal, overburden, and carbonaceous shale samples were carried out to determine the chemical composition and surface states. The XPS survey spectra of the samples show the presence of C_{1s}, O_{1s}, S_{2p}, and Fe_{2p}

as shown in Fig. 8a–i. The high-resolution Fe_{2p} XPS deconvoluted spectra shows that the Fe_{2p} XPS peak splits into two main peaks which are located at 710 eV (Fe²⁺), and 725 eV (Fe³⁺) for all the samples (Fig. 8b, e, j). Moreover, the Fe_{2p} XPS peak splits into three main peaks, which are located at 710 eV (Fe²⁺), 718 (Fe₂O₃), and 725 eV (Fe³⁺) for

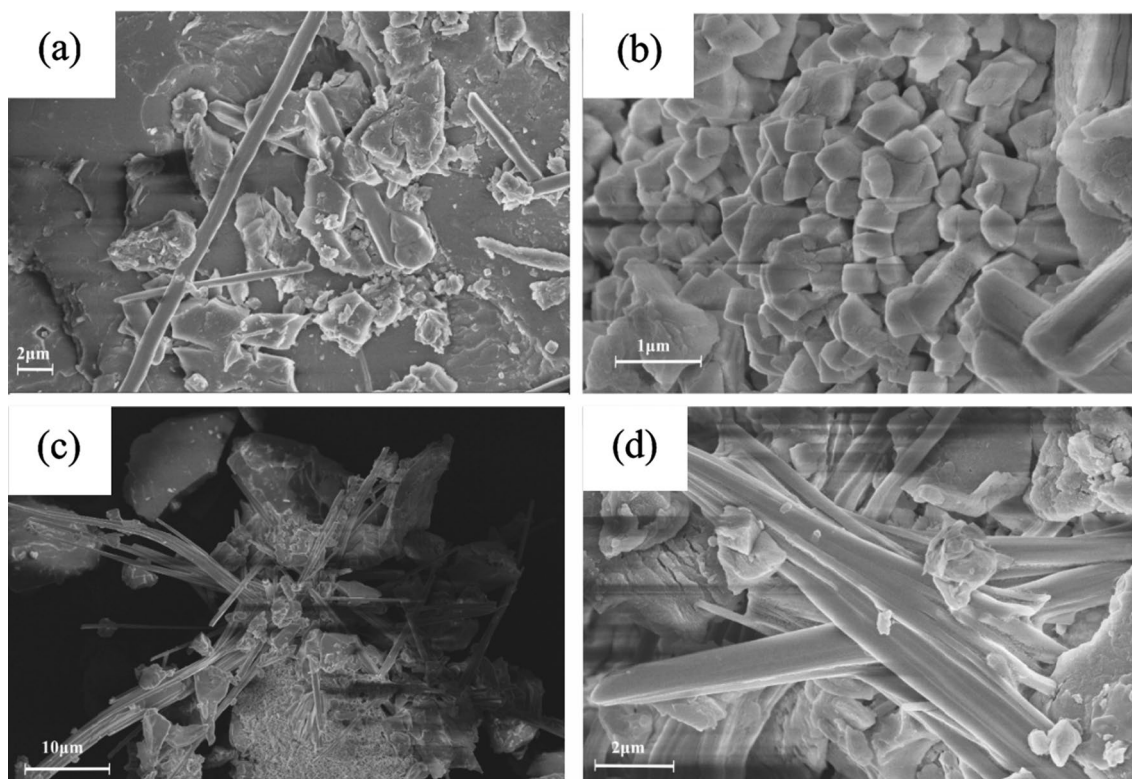


Fig. 7 SEM micrographs of **a, c** NBTP 1, **b** NBTP 2 and **d** NBTP 3 samples. Micrograph **b** denotes cubic morphology in the matrix; **a, c** and **d** shows long prismatic to needle-shaped gypsum crystals, clay minerals, Fe-hydroxides (mostly weathering products)

TPC sample as seen in Fig. 8b. The high-resolution S_{2p} XPS deconvoluted spectra shows that the S_{2p} XPS peak for all the samples are located at about 163 eV (FeS_2), and 168 eV (SO_4^{2-}), respectively (Fig. 8c, f, h). From the high-resolution S_{2p} XPS deconvoluted spectra, we can see that for TPC sample the intensity of binding energy for FeS_2 possess higher intensity than that of SO_4^{2-} , while for TPOB-20 and TPOB-60, SO_4^{2-} possesses higher intensity of binding energy than that of FeS_2 .

3.8 Correlation analysis of trace and rare earth elements (REY)

The possible source of trace elements and REEs in coal and MOB were qualitatively determined with the Pearson correlation coefficient techniques. This analysis also shows the relationship among the elements and REEs in both coal and MOB samples. A statistical tool for the data analysis (STHDA, R-software) method was used to determine the correlation coefficient (r) for the elements and REEs concentrations obtained from coal, MOB, and soil samples of Makum coalfield of India. In this study,

the significant and strong relationship of Nb is observed ($r > 0.8$) among Ti, Zr, Cr, and As. Niobium is also positively correlated with other trace elements. This strong relationship indicates similar source of origin of these elements. Irregularly scattered patches of clay minerals have been reported in the coal from Tikak Parbat formation, which may be responsible for the presence of Nb, Zr, Li, Ba, and V in coal and MOB samples. Clay minerals are expected to contribute to the emissions of trace elements of environmental importance, mainly Cr, V, and Zn to a lesser amount. Cobalt shows very strong relationship with Ni ($r = 0.97$), which is supposed to form Cobalt-organic complexes. The significant relationship ($r = 0.71$) of Cr and Ni indicates that Ni might be partly linked with clay minerals. Copper also shows strong relationship ($r > 0.8$) with Co, Ni, and As, and is also positively correlated with all other trace elements (Fig. 9). This correlation indicates that they (Co, Ni, As, and Cu) are associated with pyrite mineral as they have strong affinity towards pyrite. Copper is mainly associated with mineral matter as chalcopyrite which is a common sulphide mineral in the coal. Figure 10 shows

Table 5 Summary of the elemental distribution (ppm) in coal, MOB, and shale samples from Makum coalfield, Margherita analyzed by ICP-MS techniques

Element	TPC-20	TPC-60	TPOB-20	TPOB-60	TPCS	TPM-1	NBTP-1
Al	660	1152	40,032	43,203	45,802	1152	195
As	ND	ND	9.014	24.113	17.626	ND	0.06
B	46.4	27	23.6	46.3	29.2	27	0.2
Ba	12.4	11.9	141	131	147	11.9	ND
Ca	57.8	340	540	540	3252	340	537
Ce	2.2	1.9	4.9	3.9	7.1	2	0.1
Co	0.72	2	15.2	9.7	20.1	2	6.9
Cr	ND	ND	90.4	110	102	ND	0.67
Cu	1.7	1.7	25.1	28.9	32.2	3.4	4.4
Er	ND	ND	ND	ND	ND	ND	0.07
Eu	ND	ND	ND	ND	ND	ND	0.03
Fe	895	897	19,229	9911	33,466	897	752
Gd	0.7	0.2	6	3.4	11.4	0.3	0.3
Ho	ND	ND	ND	ND	ND	ND	0.01
K	45.4	236	22,693	37,280	22,123	236	2.7
La	1	1	10.5	7.5	17.4	1	1
Li	ND	ND	28.6	25.1	23.7	ND	0.2
Lu	ND	ND	1.07	0.48	1.56	ND	0.05
Mg	51.1	205	1473	617	3064	205	> 1758
Mn	11.7	28	258	4.3	190	28	191
Na	ND	ND	ND	ND	378	ND	27
Nb	ND	1.2	9.8	10.1	10.1	1.2	ND
Nd	ND	ND	ND	ND	ND	ND	0.21
Ni	ND	ND	584	540	3252	ND	41.9
P	4.8	ND	266	272	215	ND	2.03
Pr	ND	ND	64.8	35.4	116	ND	3.6
Sc	2.4	0.2	5.5	3.9	9.8	0.2	1.1
Si	768	1609	134,026	136,774	128,629	1609	33.2
Sm	ND	ND	ND	ND	ND	ND	0.08
Sr	23.9	43.3	64.4	36.2	73.2	43.3	0.72
Th	ND	ND	ND	1.7	4.5	ND	0.11
Ti	16	40.13	4034	4528	3997	40.13	ND
V	ND	ND	69.8	94	68.3	ND	0.02
Y	4.5	1	4.7	2.9	10.7	0.97	0.7
Yb	0.2	ND	0.2	ND	0.9	ND	0.1
Zn	ND	ND	19.31	14.47	28.11	ND	20.66
Zr	38.7	38.9	69.1	75.9	66.9	38.9	ND

the co-relationship of REEs in coal, MOB, and sediment samples. The study reveals increased concentrations of elements (in ppm) in the coal samples, with V, Cr, Ni, Cu, and Zn content in coal being considerably enriched compared to world-average concentrations (Ketris and Yudovich 2009), while Ba, As, Sc, Y, Gd, Dy, Er, Lu, and Yb concentrations are low. Tables 4 and 5 emphasises the comparison of trace and REE values to global average concentrations. Praseodymium concentrations are greater in TPS and TPOB. Only one sample, NBTP 1, had a high concentration of Nd. Relative higher concentrations of Ce, La, and Y suggest a link with terrigenous material

influx. The key factors affecting the concentration of elements in coal relate to the coal forming environment as evidenced by the kind and provenance of the sediment that provided information on terrigenous deposits (Dai et al. 2005, 2012).

4 Conclusions

A thorough investigation is carried out by combining analytical methods that include sophisticated mineralogical techniques such as XRD, XPS, SEM, and ICP-MS

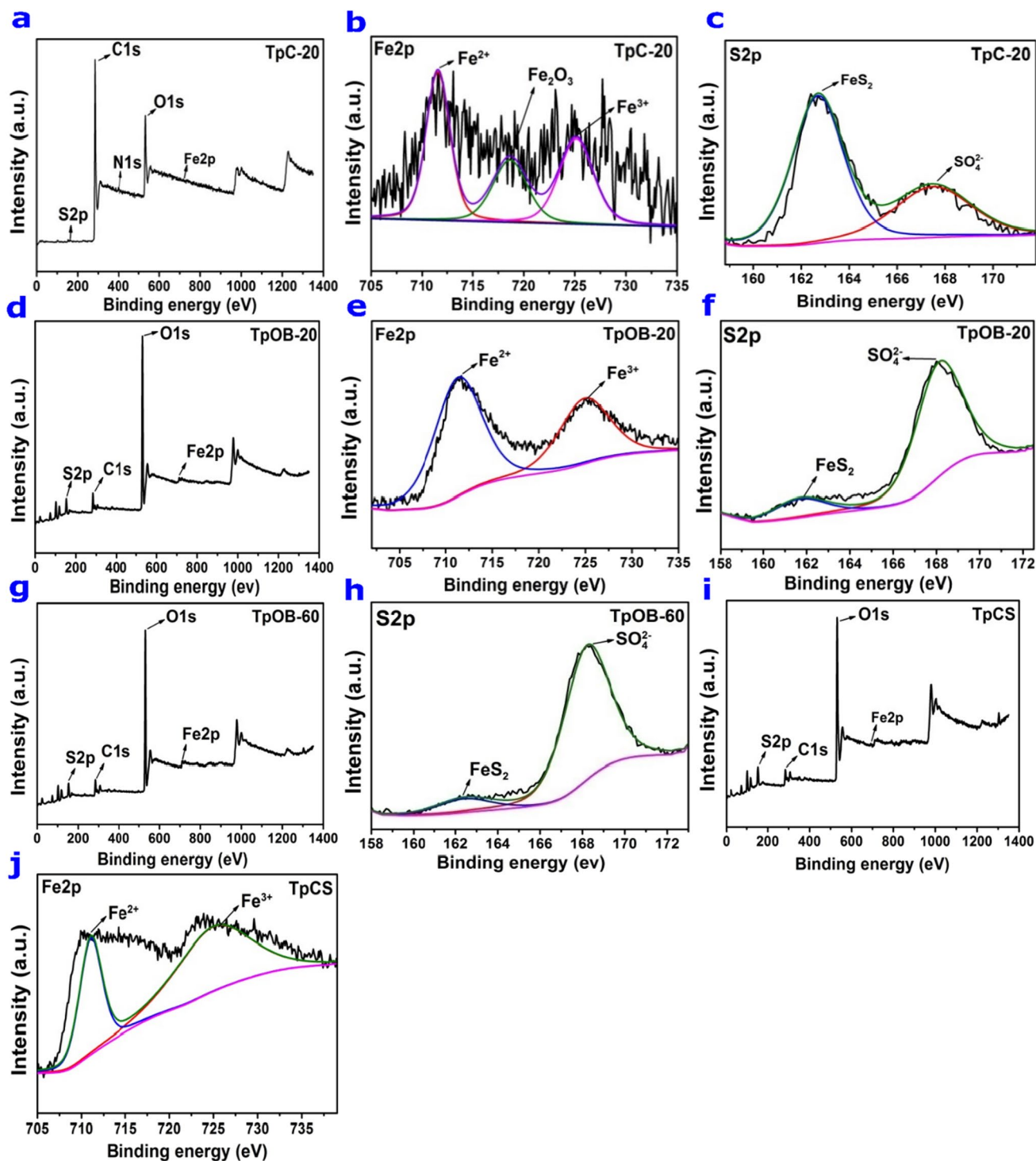


Fig. 8 The XPS survey spectra of the samples show the presence of C_{1s} , O_{1s} , S_{2p} , and Fe_{2p} (a, d, g, i); the Fe_{2p} XPS peak splits into two main peaks which are located at 710 eV (Fe^{2+}), and 725 eV (Fe^{3+}) for all the samples (b, e, j)

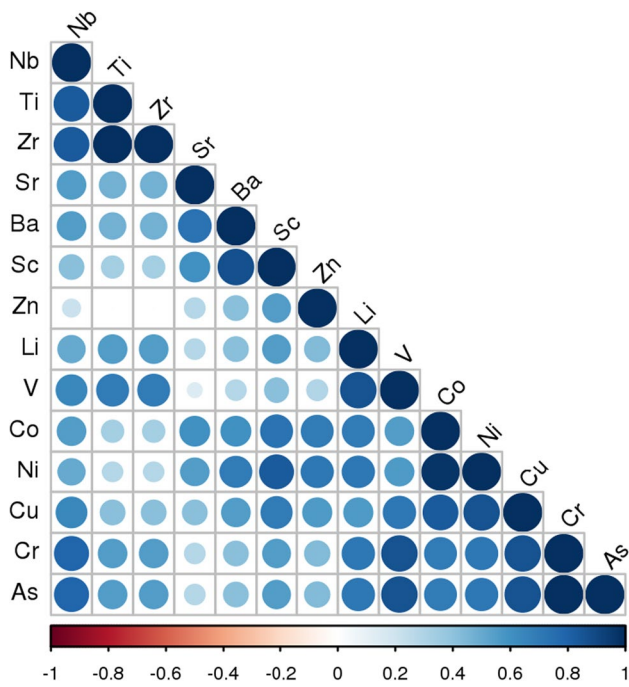


Fig. 9 Pearson's correlation coefficient of trace elements coal, MOB, and shale samples

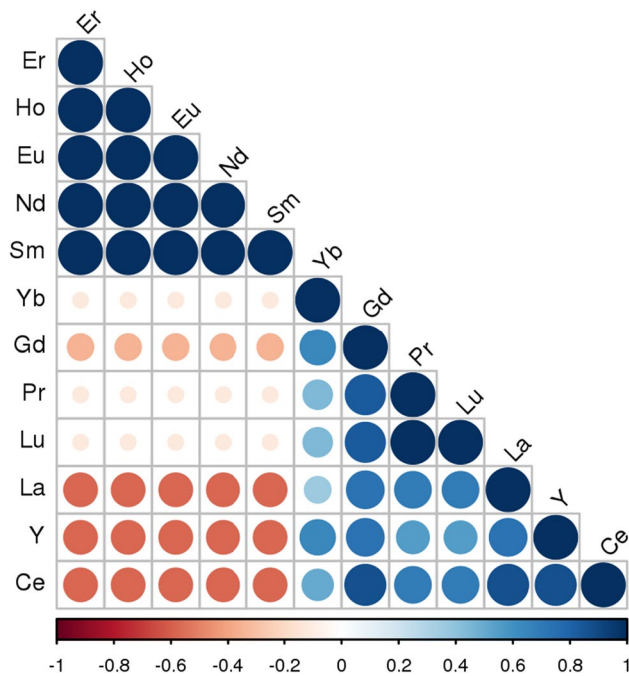


Fig. 10 Pearson's correlation coefficient of REEs in coal, MOB, and shale samples

examination of coal, shale, and MOB samples. Clay minerals, quartz, pyrite, calcite, and haematite were discovered in Makum coal and MOB samples. Petrographic analysis is a potent investigative method for determining the amount of macerals assemblages in coal samples and evaluating their process circumstances. The carbon content of the shale sample under inquiry was discovered to be quite high, signifying that it is a carbonaceous shale that requires additional investigation. The existence of trace and significant REY is observed in all three categories of samples. The presence of aliphatic amino (NH) and aromatic C=C groups, as well as S-S and C-S, C-O-C, C-H, and SO₄²⁻ functional groups, is revealed by FTIR analysis. The petrology study revealed a high concentration of sulphide minerals, as well as a variety of maceral compositions, which may imply a time of pyrite mineralization supported by organic matter (macerals). This study suggest that the coal is high volatile B bituminous, which is typical of coal from Northeast India. The composition of the macerals is comparable to one of India's largest coal reserves. During the sulfur analysis, the investigation discovered the presence of a moderate amount of sulfur. This study reveals increased concentrations of potentially hazardous elements (in ppm) in the coal samples, with V, Cr, Ni, Cu, and Zn content in coal being considerably enriched compared to world-average concentrations. The overall mineralogical and geochemical investigation presented in this study will be effective in designing the mitigation processes for the environmental consequences like acid mine water generation in the coal mining area and also provides a new avenue for the further investigation on gainful and sustainable recovery of REEs from coal, MOB, and shale samples of Makum coalfield.

Acknowledgements Authors express thanks to the Director, CSIR-North East Institute of Science & Technology, Jorhat for permission to conduct the study. Special thanks to MoES (Govt of India) for his financial assistance to our project (GPP364). Authors are thankful to SAIF, IIT-Bombay for ICPMS analysis of the samples.

Funding Funding was provided by Binoy K. Saikia (Ministry of Earth Science).

Declarations

Competing interests The authors declare no competing financial interest.

Open Access This article is licensed under a Creative Commons Attribution 4.0 International License, which permits use, sharing, adaptation, distribution and reproduction in any medium or format, as long as you give appropriate credit to the original author(s) and the source, provide a link to the Creative Commons licence, and indicate if changes were made. The images or other third party material in this article are included in the article's Creative Commons licence, unless indicated otherwise in a credit line to the material. If material is not included in

the article's Creative Commons licence and your intended use is not permitted by statutory regulation or exceeds the permitted use, you will need to obtain permission directly from the copyright holder. To view a copy of this licence, visit <http://creativecommons.org/licenses/by/4.0/>.

References

- Ahmed M (1996) Petrology of Oligocene coal Makum coalfield Assam northeast India. *Int J Coal Geol* 30(4):319–325
- ASTM (2002) Annual book of ASTM standards D3177–02 (Reapproved 2007) Test methods for total sulfur in the analysis sample of coal and coke. ASTM International, West Conshohocken
- ASTM (2010) Annual book of ASTM standards D2234M Standard practice for collection of a gross sample of coal. ASTM International, West Conshohocken
- ASTM (2011a) Annual book of ASTM standards D3173–11 test method for moisture in the analysis sample of coal and coke. ASTM International, West Conshohocken
- ASTM (2011b) Annual book of ASTM standards D3174–11 test method for Ash in the analysis sample of coal and coke. ASTM International, West Conshohocken
- ASTM (2011c) Annual book of ASTM standards D3175–11 test method for volatile matter in the analysis sample of coal and coke. ASTM International, West Conshohocken
- ASTM standard D2789-11a (2011) Determination of forms of sulfur in coal [Evaluation of ASTM Standard Methods D-2492 and D-3177]. *Energy Sources (United States)* 3(2)
- ASTM D6357-21b (2021) Standard test methods for determination of trace elements in coal coke and combustion residues from coal utilization processes by inductively coupled plasma atomic emission spectrometry inductively coupled plasma mass spectrometry and graphite fur. ASTM International, West Conshohocken
- Barooah PK, Baruah MK (1996) Sulfur in Assam coal. *Fuel Process Technol* 46(2):83–97
- Baruah BP, Khare P (2010) Mobility of trace and potentially harmful elements in the environment from high sulfur Indian coal mines. *Appl Geochem* 25(11):1621–1631
- Chou CL (2012) Sulfur in coals: a review of geochemistry and origins. *Int J Coal Geol* 100:1–13
- Dai S, Ren D, Tang Y, Yue M, Hao L (2005) Concentration and distribution of elements in Late Permian coals from western Guizhou Province China. *Int J Coal Geol* 61(1–2):119–137
- Dai S, Ren D, Chou CL, Finkelman RB, Seredin VV, Zhou Y (2012) Geochemistry of trace elements in Chinese coals: a review of abundances genetic types impacts on human health and industrial utilization. *Int J Coal Geol* 94:3–21
- Dai S, Bechtel A, Eble CF, Flores RM, French D, Graham IT, Hood DM, Hower JC, Korasidis VK, Moore TA, Wei Q, Zhao L, O'Keefe JM (2020) Recognition of peat depositional environments in coal: a review. *Int J Coal Geol* 219:103383
- Dutta M, Saikia J, Taffarel SR, Waanders FB, DeMedeiros D, Cutruneo CM, Silva LF, Saikia BK (2017) Environmental assessment and nano-mineralogical characterization of coal overburden and sediment from Indian coal mining acid drainage. *Geosci Front* 8(6):1285–1297
- Dutta M, Islam N, Rabha S, Narzary B, Bordoloi M, Saikia D, Silva LF, Saikia BK (2020) Acid mine drainage in an Indian high-sulfur coal mining area: Cytotoxicity assay and remediation study. *J Hazard Mater* 389:121851
- Evans P (1932) The Tertiary succession in Assam: geology and metallurgy institute of India. *Trana Mineral* 27:155–260
- Greb SF, Eble CF, Chesnut DR Jr (2002) Comparison of the Eastern and Western Kentucky coal fields (Pennsylvanian) USA—why are coal distribution patterns and sulfur contents so different in these coal fields? *Int J Coal Geol* 50(1–4):89–118
- Indian Bureau of Mines (IBM) (2001) Annual Report Ministry of Steel and Mines Govt of India
- International Committee for Coal and Organic Petrology (ICCP) (1998) The new vitrinite classification (ICCP System 1994). *Fuel* 77:349–358
- International Committee for Coal and Organic Petrology (ICCP) (2001) The new inertinite classification (ICCP System 1994). *Fuel* 80:459–471
- International Energy Agency (IEA) (2020) <https://www.iea.org/reports/coal-2020>. Accessed 30 Dec 2022
- International Energy Agency (IEA) (2022) <https://iea.blob.core.windows.net/assets/91982b4e-26dc-41d5-88b1-4c47ea436882/Coal2022.pdf>
- Islam N, Rabha S, Silva LFO, Saikia BK (2019) Air quality and PM10-associated poly-aromatic hydrocarbons around the railway traffic area: statistical and air mass trajectory approaches. *Environ Geochem Health* 41(5):2039–2053
- Islam N, Dihingia A, Khare P, Saikia BK (2020) Atmospheric particulate matters in an Indian urban area: health implications from potentially hazardous elements, cytotoxicity, and genotoxicity studies. *J Hazard Mater* 384:121472
- Islam N, Rabha S, Subramanyam KSV, Saikia BK (2021) Geochemistry and mineralogy of coal mine overburden (waste): a study towards their environmental implications. *Chemosphere* 274:129736
- Juwarkar AA, Jambhulkar HP (2008) Phytoremediation of coal mine spoil dump through integrated biotechnological approach. *Biores Technol* 99(11):4732–4741
- Ketris MÁ, Yudovich YE (2009) Estimations of Clarks for Carbonaceous biolithes: world averages for trace element contents in black shales and coals. *Int J Coal Geol* 78(2):135–148
- Mukherjee S, Srivastava SK (2005) Trace elements in high-sulfur Assam coals from the makum coalfield in the Northeastern Region of India. *Energy Fuels* 19(3):882–891
- Mukherjee KN, Dutta NR, Chandra D, Singh MP (1992) Geochemistry of trace elements of tertiary coals of India. *Int J Coal Geol* 20(1–2):99–113
- Oxford Analytica (2017) Foul fundamentals will curb world coal. *Emerald Expert Briefings (oxan-db)*
- Pickel W, Kus J, Flores D, Kalaizidis S, Christanis K, Cardott BJ, Miskennan M, Rodrigues S, Hentschel A, Hamor-Vido M, Crosdale P, Wagner N (1994) ICCP 2017 Classification of liptinite—ICCP system. *Int J Coal Geol* 169:40–61
- Rabha S, Saikia J, Subramanyam KSV, Hower JC, Hood MM, Khare P, Saikia BK (2018) Geochemistry and nanomineralogy of feed coals and their coal combustion residues from two different coal-based industries in northeast India. *Energy Fuels* 32(3):3697–3708
- Raja Rao CS (1981) Coalfields of India. G.S.I., Bull.Series-A, No. 45(1), Coalfields of North Eastern India, 75 p
- Saikia BK, Ward CR, Oliveira ML, Hower JC, De Leao F, Johnston MN, Sharma A, Baruah BP, Silva LF (2015a) Geochemistry and nano-mineralogy of feed coal mines overburden and coal-derived fly ashes from Assam (North-east India): a multi-faceted analytical approach. *Int J Coal Geol* 137:19–37
- Saikia BK, Wang P, Saikia A, Song H, Liu J, Wei J, Gupta UN (2015b) Mineralogical and elemental analysis of some high-sulfur Indian Paleogene Coals: a statistical approach. *Energy Fuels* 29(3):1407–1420
- Saikia BK, Saikia A, Choudhury R, Xie P, Liu J, Das T, Dekaboruah HP (2016) Elemental geochemistry and mineralogy of coals and associated coal mine overburden from Makum coalfield (Northeast India). *Environ Earth Sci* 75(8):1–21
- Saikia BK, Saikia J, Rabha S, Silva LF, Finkelman R (2018) Ambient nanoparticles/nanominerals and hazardous elements from coal combustion activity: implications on energy challenges and health hazards. *Geosci Front* 9(3):863–875

- Senapaty A, Behera P (2015) Stratigraphic control of petrography and chemical composition of the lower gondwana coals Ib-valley coalfield, Odisha, India. *J. Geosci. Environ. Protect.* 3(04):56
- Solaymani Z, Taghipour N (2012) Petrographic characteristics and palaeoenvironmental setting of Upper Triassic Olang coal deposits in Northeastern Iran. *Int J Coal Geol* 92:82–89
- Spears DA (2000) Role of clay minerals in UK coal combustion. *Appl Clay Sci* 16(1–2):87–95
- Suárez-Ruiz I, Ward CR (2008) Basic factors controlling coal quality and technological behavior of coal In *Applied coal petrology*. Elsevier, Amsterdam, pp 19–59
- Suwarna N (2006) Permian Mengkarang coal facies and environment based on organic petrology study. *Indones J Geosci* 1(1):1–8
- Turner BR, Richardson D (2004) Geological controls on the sulphur content of coal seams in the Northumberland Coalfield Northeast England. *Int J Coal Geol* 60(2–4):169–196
- Ward CR, Gurba LW (1998) Occurrence and distribution of organic sulphur in macerals of Australian coals using electron microprobe techniques. *Org Geochem* 28(11):635–647

Publisher's Note Springer Nature remains neutral with regard to jurisdictional claims in published maps and institutional affiliations.